Kinetic oscillations in the NO+CO reaction on the Pt(100) surface: An alternative reaction mechanism

S. J. Alas, S. Cordero, and I. Kornhauser
Departamento de Química, Universidad Autónoma Metropolitana, Iztapalapa, P.O. Box 55-534, México, Distrito Federal, Mexico

G. Zgrablich[a)]
Laboratorio de Ciencias de Superficies y Medios Porosos, Universidad Nacional de San Luis, 5700 San Luis, Argentina

(Received 26 August 2004; accepted 1 February 2005; published online 12 April 2005)

Kinetic oscillations in the catalytic reduction of NO by CO on a reconstructing Pt(100) surface are simulated by using a dynamic Monte Carlo method. The simulation is based on the HS model and takes into account an alternative reaction mechanism arising from recent experimental findings for the catalytic reduction of No on Rh(111), which replaces the classical N+N recombination step by the formation of a $(N–NO)^*$ intermediary species for the production of molecular nitrogen. A synchronized mechanism and spatiotemporal patterns are observed during the oscillations. Oscillations are analyzed in terms of the controlling parameters involved in the reaction mechanism. Different values of these parameters lead to sustained, attenuated, and modulated oscillations. © *2005 American Institute of Physics*. [DOI: 10.1063/1.1878572]

I. INTRODUCTION

The NO reduction by CO reaction on Pt(100) surfaces has been extensively studied, both experimentally and theoretically, during the past years under UHV conditions and relatively high temperatures.[1–14] This reaction is very important in view of the interest to develop improved catalysts for atmospheric pollution-control processes through the decrease of NO_x emissions. On the other hand, the dynamic behavior that the above reaction displays during the different stages of the catalytic process presents interesting theoretical problems, in particular, the determination of the conditions for kinetic oscillations and the formation of reaction patterns.

The catalytic reduction of NO by CO proceeds according to the global reaction:

$$NO + CO \rightarrow CO_2 + 1/2N_2.$$

Experimentally, it has been observed that this reaction presents kinetic oscillations as well as spatiotemporal pattern formation. On a Pt(100) surface, these phenomena arise at pressure and temperature ranges of around 10^{-6}–10^{-4} Pa and 400–500 K, respectively.[1–4] It is known that a clean Pt(100) surface in its more stable state exhibits a quasihexagonal arrangement (hex) of Pt atoms which can be transformed into a square arrangement (1×1) by deposition of adsorbate molecules such as NO or CO. The interaction between the surface and adsorbate molecules can then lead to a phase transition of the type: hex$\leftrightarrows1\times1$. At $T<450$ K, the Pt(100) surface is stable and the oscillations are entirely driven by an autocatalytic reaction between coadsorbed NO and CO on the square phase; while at higher temperatures, the hex$\leftrightarrows1\times1$ phase transition is directly involved in the surface oscillations.[1–11] The conventional mechanism of NO reduction by CO on the Pt(100) surface that has been employed consists of the following reaction steps:

$$CO_{(gas)} + \text{site} \leftrightarrows CO_{(ads)}, \tag{1}$$

$$NO_{(gas)} + \text{site} \leftrightarrows NO_{(ads)}, \tag{2}$$

$$NO_{(ads)} + \text{site} \rightarrow N_{(ads)} + O_{(ads)}, \tag{3}$$

$$N_{(ads)} + N_{(ads)} \rightarrow N_{2(gas)} + 2\ \text{sites}, \tag{4}$$

$$NO_{(ads)} + N_{(ads)} \rightarrow N_2O_{(gas)} + 2\ \text{sites}, \tag{5}$$

$$CO_{(ads)} + O_{(ads)} \rightarrow CO_{2(gas)} + 2\ \text{sites}. \tag{6}$$

Under this scheme, the production of N_2 occurs via the recombination of two adsorbed N atoms. Previous investigations have found that the formation of products depends on the rate of dissociation of NO. This dissociation is totally functional on the 1×1 phase while it is rather negligible on the hex phase of the Pt(100) surface.[2,3,7]

Theoretical procedures have been implemented to try to explain the experimental behavior of the system. Two kinds of approaches have been mainly used: kinetic equations derived from mean field approximations and Monte Carlo (MC) methods.[3–14] In the latter case, the behavior of the catalytic system can be simulated in real time units by using dynamic Monte Carlo (DMC) techniques.[15]

Recent molecular beam studies on the reduction of NO over Rh(111) (Refs. 16–21) have indicated that the standard reaction scheme presented above needs to be modified at least in one of its reaction steps. It was found that when a ^{14}N-covered Rh(111) surface is exposed to a $^{15}NO+CO$ beam, the molecular nitrogen that is being produced always

[a)]Author to whom correspondence should be addressed. Electronic mail: giorgio@unsl.edu.ar

contains at least one ^{15}N atom.[16,17] This experimental finding means that the nitrogen recombination, step (4) which is usually assumed as responsible of the formation of molecular nitrogen, is in fact not fast enough to account for the N_2 production under typical reaction conditions. Instead, an intermediate species is formed via the interaction of adsorbed atomic nitrogen with undissociated adsorbed NO molecules. The resulting $(N–NO)^*$ species may then either decompose to $N_{2(gas)}+O_{(ads)}$ or just simply desorbs in the molecular form.

These results suggest a new hypothesis which is worthy of being investigated, since the new reaction characteristics observed on the Rh(111) surface could be also occurring on a metallic surface involving a (100) face which experiences a hex$\leftrightarrows 1\times 1$ phase reconstruction such as that arising on the Pt(100) surface.

The purpose of the present work is to perform DMC simulations of the NO+CO reaction system on a Pt(100) surface by introducing the new findings concerning the reaction mechanism. In particular, we consider important to explore under which conditions an oscillation behavior can be obtained and which are the dominant parameters controlling the reaction.

II. MODEL AND SIMULATION METHOD

Our analysis is based on the HS model, which has two variants: the hollow-site model and the top-site model, in this work the later approach is chosen. This model was proposed by Gelten *et al.*[22] for the $CO+O_2$ reaction on a Pt(100) surface; we believe that a similar method can also be applied to the NO+CO reaction. Briefly, in our simulations, the surface of a Pt(100) single crystal is represented as a regular grid with periodic boundary conditions, which consists of $L\times L$ unit cells divided in two sites: site 1 and site 2. Site 1 corresponds either to a vacant site or to an adsorbed particle and site 2 is used as a phase label for both hexagonal and square phases. The detailed description of the model can be found in reference.[22]

Our simulations, which correspond to the DMC type, follow the dynamic behavior of the system, which is determined by the master equation:

$$\frac{\partial P_\alpha}{\partial t}=\sum_\beta (W_{\beta\to\alpha}P_\beta - W_{\alpha\to\beta}P_\alpha), \tag{7}$$

where P_α and P_β are the probabilities to find the system in the configurations α and β, respectively. $W_{\beta\to\alpha}$ and $W_{\alpha\to\beta}$ are the transition probabilities per unit time for the different reactions such as adsorption, desorption, etc. We note, that this equation simply expresses a balance among the probabilities of the system evolving from the α configuration to the β configuration and vice versa.

The simulation of the process determined by Eq. (7) may be carried out through different methods.[23] We have chosen the following one: we select a site at random with probability $1/N$, where N represents the total number of sites; afterwards, a reaction step i is selected at random with probability W_i/R, where W_i is the rate of transition of chosen reaction step, and R is the sum of all the possible transitions, i.e., the total-transition rate of the system. If the selected reaction step i is feasible on the chosen site then it is executed. After each site is selected, the time is incremented by Δt according to

$$\Delta t=-\frac{\ln \xi}{NR}, \tag{8}$$

where ξ is a random number selected uniformly in the interval (0,1). This equation renders the real time caused by a transition of the system; in other words, Eq. (8) establishes the relation between the "arbitrary MC time" and the real time of the system.

On the other hand, we propose the following general reaction scheme that includes the new experimental evidence found on the Rh(111) surface:[20]

$$CO_{(gas)}+\text{site}\leftrightarrows CO_{(ads)}, \tag{9}$$

$$NO_{(gas)}+\text{site}\leftrightarrows NO_{(ads)}, \tag{10}$$

$$NO_{(ads)}+\text{site}\to N_{(ads)}+O_{(ads)}, \tag{11}$$

$$NO_{(ads)}+N_{(ads)}\to (N–NO)^*+\text{site}, \tag{12}$$

$$(N\text{-}NO)^*\to N_{2(gas)}+O_{(ads)}, \tag{13}$$

$$CO_{(ads)}+O_{(ads)}\to CO_{2(gas)}+2\ \text{sites}, \tag{14}$$

where $(N–NO)^*$ is the activated complex intermediate. Note that we have eliminated the classical N+N recombination step for the production of N_2 and replaced it by the alternative step going through the formation of the $(N–NO)^*$ species. Therefore, we are not adding an additional feedback loop to the reaction mechanism, but simply replacing one by another. In addition, the surface diffusion of adsorbed NO and CO species is also considered.

The number of steps involved in the previous mechanism is relatively large. We have not taken into account the production of N_2O given that its rate is expected to be low compared to that corresponding to N_2.[1] Moreover, it is known that on the Pt(100) surface there exist different site densities between the hexagonal and the 1×1 phase, the difference being $\approx 20\%$.[3] In our case this factor is ignored, so the densities of Pt atoms both on the hexagonal and the 1×1 phases are assumed to be the same. For the sake of simplicity, lateral interactions among different particles adsorbed on both phases are neglected, although effects of these interactions have been observed in experimental studies.[24,25]

The above restrictions make our simulation easier to perform. The main elementary reaction steps to be taken into account are the following.

A. Adsorption

A molecule of NO or CO is chosen from the gas phase, according to the corresponding flux given by the Hertz–Knudsen equation:

$$J_i = \frac{p_i}{(2\pi m_i kT)^{1/2}}, \tag{15}$$

where J_i is the flux of NO or CO molecules $m^{-2}\,s^{-1}$, p_i is the partial pressure, m_i is the molar mass of NO or CO, k is the Boltzmann constant, and T is the absolute temperature. The adsorption rate W_i of particles impinging on the surface per site and per second is then obtained as

$$W_i = J_i \times A \times S_0, \tag{16}$$

where A is the number of sites per square meter of surface, in this case of Pt(100), and S_0 is the initial sticking coefficient.

In our simulation CO adsorption occurs on both hexagonal and 1×1 phases; for the sake of simplicity we consider the same CO adsorption rate on both phases. It is, however, pertinent to mention that experiments show that these two rates are in fact different.[25] NO adsorption takes place only on the 1×1 phase; we have made this assumption based on the fact that NO can be only dissociated in this phase;[3,7] again, in a real system NO adsorbs on both phases.[24]

After a type of molecule is chosen a unit cell is immediately selected at random, if this cell is vacant the molecule can be absorbed, otherwise the trial is rejected.

B. Desorption

Again, a unit cell is chosen at random, if it is occupied either by NO or CO and the appropriate reaction step has been chosen, the molecule desorbs to the gas phase otherwise the trial ends. Desorption is considered as an activated process with a rate given by

$$W_i = \upsilon_i \exp(-E_{ai}/kT), \tag{17}$$

where υ_i is the frequency factor and E_{ai} the activation energy for species i.

CO desorption occurs both from the hexagonal and 1×1 phases at the same rate; actually, experiments indicate that these rates are different.[3,7]

C. Diffusion

A unit cell on the surface is picked at random, if it is occupied by NO or CO, there is a nearest-neighbor (nn) unit cell unoccupied and the appropriate reaction step has been chosen, then the molecule is moved to the vacant unit cell, otherwise the trial ends. The diffusion rate W_i is obtained directly as a frequency factor υ_i. In the simulation the diffusion of CO molecules can be performed across phase boundaries.

D. No dissociation

On a Pt(100) surface this process can only occur on the 1×1 phase. The dissociation process starts by selecting a unit cell at random, if NO already occupies this cage, if it has a nn vacant unit cell and if the appropriate reaction step has been chosen, then the NO particle dissociates into atomic N and O adsorbed species, respectively. The dissociation rate is calculated as an activated process, as in Eq. (17), with appropriate frequency factor and activation energy.

E. N_2 production

This reaction is possible whenever the formation of an intermediate (see reaction scheme steps 12 and 13) takes place. A unit cell is chosen at random, if this site is occupied by NO (or N), if it has a nn unit cell occupied by N (or NO) and if the appropriate reaction step has been chosen, then the formation of the $(N–NO)^*$ intermediary species is achieved; this event causes the immediate production of N_2 and its desorption to the gas phase, leaving an O species adsorbed on the surface. The former is considered as an activated process with appropriate frequency factor and activation energy and occurs rapidly according to experimental observations.[7] This reaction can take place across phase boundaries.

F. CO_2 production

The process starts again by randomly selecting a unit cell. If it is occupied by CO (or O) and has a nn unit cell occupied by O (or CO), and if the appropriate process step has been chosen, then CO_2 is produced and desorbed immediately after its formation. As in the case of N_2 production, this is considered as an activated process and can happen across phase boundaries.

G. Surface reconstruction

Experimental results indicate that the hex$\rightarrow1\times1$ phase transition occurs by nucleation and trapping of the CO molecules on the Pt(100) surface; this transformation of the surface is caused by the different heats of adsorption of CO on both phases, which is considerably higher on the unreconstructed 1×1 phase than on the reconstructed hexagonal one.[25–28] The observations show that four to five CO molecules are involved in the restructuring process.[29] Thiel *et al.* proposed that this transformation occurs by a sequential mechanism: initially, the 1×1 phase is formed by nucleation of CO adsorbed molecules on a precursory hexagonal phase, this is followed by the migration and trapping of the CO molecules by way of growing islands.[27]

Incorporating these experimental results into our model, we assume the following two mechanisms: (i) the *nucleation* mechanism for the hex$\rightarrow1\times1$ reconstruction takes place if there exist five CO adsorbed molecules forming a nucleating cluster; (ii) island growth on the square phase happens through a *trapping* mechanism, i.e., when one CO molecule is found on the hexagonal phase and if it has as nn any of the molecules forming CO, NO, or a CO/NO mixture islands on the 1×1 phase, then the CO molecule is trapped into that island and its unit cell reconstructs from the hexagonal to the square phase. The fact that a growing island can be made by CO and NO is based on experimental evidence establishing that the heats of adsorption of both molecules are almost the same.[24] The rates for these two processes are determined directly by appropriate frequency factors.

The inverse $1\times1\rightarrow$hex transformation occurs in empty unit cells of the square phase. In this analysis, we only require of a unit cell to perform this transformation, which is considered as an activated process with appropriate frequency factor and activation energy.

TABLE I. Values of the parameters used in simulations and their comparison with their experimentally observed values.

Reaction	$p^{\exp}$(Pa)	p^{sim}(Pa)	$S_0^{\exp}$	S_0^{sim}	References
CO adsorption	0.4×10^{-4}	$(1–4)\times10^{-4}$	≈0.8	0.8	2,24,29
NO adsorption	4.0×10^{-4}	$(1–4)\times10^{-4}$	≈0.8	0.8	2,24
	$\nu^{\exp}(s^{-1})$	$\nu^{sim}(s^{-1})$	$E_a^{\exp}$(kJ/mol)	E_a^{sim}(kJ/mol)	
CO desorption	4×10^{12}–1×10^{15}	3×10^{13}–1×10^{15}	115–157	148–157	3,7
NO desorption	1.7×10^{14}–1.7×10^{15}	3×10^{13}–1×10^{15}	142–155	147–155	3,7
NO dissociation	1×10^{15}–2×10^{16}	1×10^{15}	117–134	123.5–132.5	3,7
N_2 production	1.3×10^{11}	1×10^{11}	84.6	84.5–88.4	7
CO_2 production	2×10^{8}–2×10^{10}	2×10^{10}	50–100	83.5	3,7,22
$1\times1\rightarrow$hex	2.5×10^{10}–2.5×10^{11}	1×10^{10}	103–107	109.8	3,7,28
CO nucleation	…	0.015–0.03	≈0	0	22, 26–29
CO trapping	…	0.015–0.03	≈0	0	22,28,29
CO diffusion	…	10–50	…	…	22
NO diffusion	…	10–50	…	…	This work

Additional details that have been included in our study are (i) previous results show that in the interval 475 K–500 K, oscillations take place as a result of the hex$\leftrightarrows1\times1$ reconstruction process,[2,3] taking into account this fact, our simulations have been performed at $T=485$ K; (ii) oxygen desorption from the 1×1 phase is neglected, since experiments indicate that this process happens above 600 K;[30] (iii) O diffusion is neglected, since this process is expected to be slower if compared to the remaining reaction steps; (iv) N diffusion is neglected in view that in our reaction scheme N_2 is produced through the formation of the N–NO intermediary, and that NO desorption and diffusion is allowed, hence N and NO species can easily meet in nn cells (in contrast, in the classical reaction scheme where N_2 is formed through the recombination of two adsorbed N atoms, N diffusion is unavoidable[10,13]).

III. RESULTS AND DISCUSSION

A large amount of calculations were performed trying to understand the effects that each of the parameters of the model exerts on the behavior of the system. Here we only present the most important results.

Table I shows a comparison between the values of the parameters used in the simulations to obtain the rate of each elementary reaction step and their experimental estimation. Unfortunately there are no available data for the rates of formation of the $(N–NO)^*$ intermediary and its subsequent decay, since this mechanism has been proposed only recently, so we have used classical experimental estimations for this rate based on the N+N mechanism.

Kinetic oscillations can be found only in a region of values of all these parameters, and in that region different types of oscillations appear depending on the values of some of these parameters. Our analysis points to the understanding of the effect of the different elementary reaction steps on the appearance of a particular behavior and to determine the parameter range of values where such behavior can be observed.

A first general result is that kinetic oscillations were observed only in the partial pressure ratio range: $1.2\leqslant p_{NO}/p_{CO}\leqslant4$. This finding agrees partially with experiments, which indicate that kinetic oscillations have been observed within $0.8<p_{NO}/p_{CO}<1.8$ and 478–490 K of partial pressure ratio and temperature ranges, respectively.[2] Three oscillatory types were found within that p_{NO}/p_{CO} range: (i) if this ratio is in the interval $1.2\leqslant p_{NO}/p_{CO}\leqslant1.5$, damped oscillations are obtained, (ii) the best sustained oscillatory pattern was found when the ratio is restricted to the following condition: $1.5\leqslant p_{NO}/p_{CO}\leqslant2$, and (iii) when the p_{NO}/p_{CO} ratio is in the range $2<p_{NO}/p_{CO}\leqslant4$, irregular oscillations were observed. On the other hand, when $p_{NO}/p_{CO}<1.2$ the surface became poisoned by CO deposited on 1×1 phase.

In view that sustained oscillations appear when $1.5\leqslant p_{NO}/p_{CO}\leqslant2$, we proceed now to examine the effect of the rate constants on the oscillatory pattern behavior in this partial pressure ratio range. Some of these rate constants are not going to be mentioned, since they have little effect on the oscillatory behavior of the system. The following situations guarantee the appearance of oscillatory patterns.

(1) Sustained oscillations can be observed when the CO and NO desorption rate constants are rather low, that is, 5.5×10^{-4} s^{-1} and 5.8×10^{-4} s^{-1}, respectively, with a NO dissociation rate constant of around 5 s^{-1}. Figure 1 shows the behavior of the rate of production of CO_2 (a), measured as turnover number (TON), i.e., the number of produced molecules per Pt atom per second, and the coverage of each species (b), measured in monolayers. If the values of the CO and NO desorption rate constants are increased, the oscillations begin to decline proportionally; a transition to damped oscillation behavior is observed when the values of the rate constants are around 15 times larger, if the values of the rate constants keep increasing from that transition point strongly damped oscillations are obtained (Fig. 2). This behavior can be understood by considering that desorption and reaction compete among them: if CO and NO desorption rates are too high, then these species are eliminated from the surface faster than their consumption through the reactions producing CO_2 and N_2.

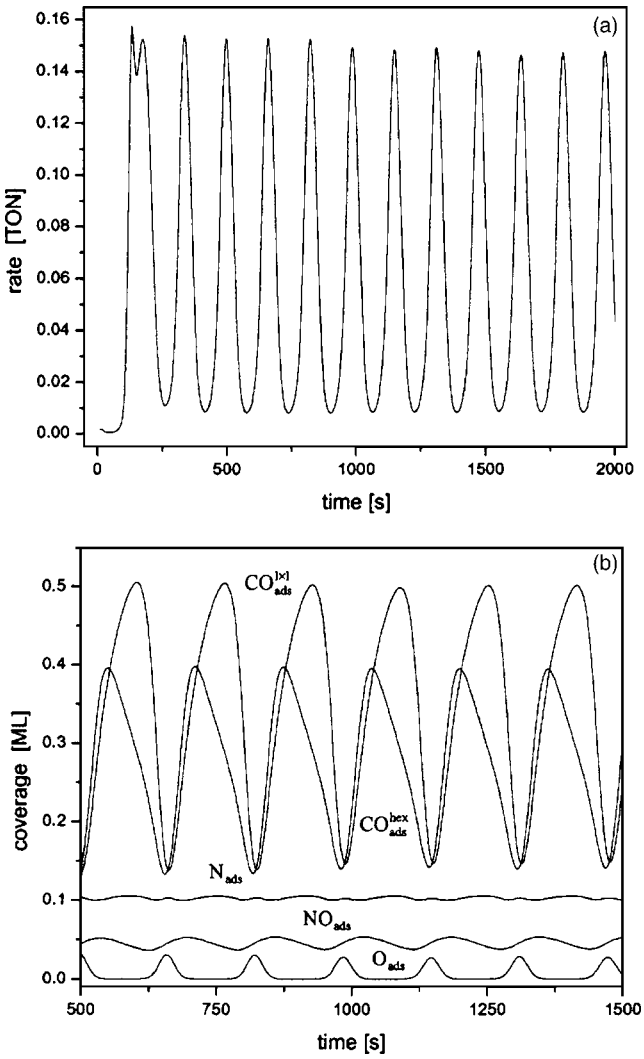

FIG. 1. Sustained oscillations: (a) CO_2 production rate in turnover number (TON); (b) CO coverage on the square and hexagonal phases (NO, N, and O coverage values are also indicated). Grid size: 1024×1024 unit cells.

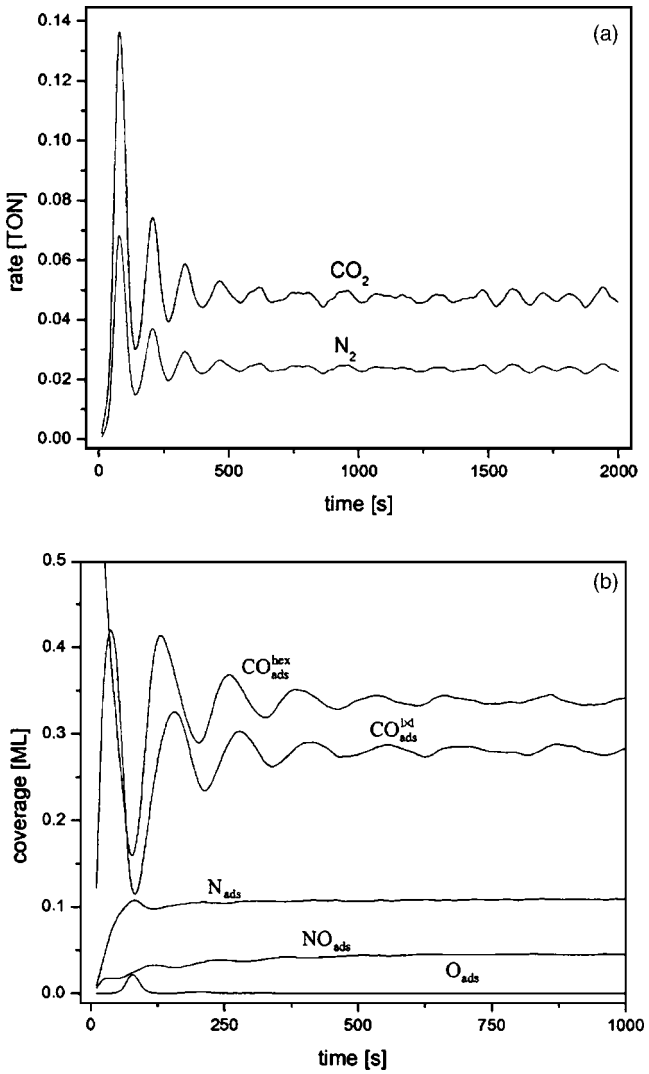

FIG. 2. Damped oscillations: (a) CO_2 and N_2 reaction rates for $W_{COdes}=1.2\times10^{-2}\ s^{-1}$ and $W_{NOdes}=2.0\times10^{-2}\ s^{-1}$; (b) coverage of adsorbed CO molecules on square and hexagonal phases (NO, N, and O coverage values are also indicated). Grid size: 512×512 unit cells.

(2) Modulated oscillations are obtained if the CO and NO desorption rate constants values are fixed ($5.5\times10^{-4}\ s^{-1}$ and $5.8\times10^{-4}\ s^{-1}$, respectively) and if the NO dissociation value is increased by a factor of 10. This novel interesting behavior is shown in Fig. 3, where we can observe that, in addition to the CO_2 production rate (a), also the coverages of CO species (b), and N species (c), present clearly modulated oscillations. The appearance of a new oscillatory behavior is usually expected when an additional negative feedback loop is added to the reaction scheme,[31] however, as explained before, this is not the case here. The explanation of this behavior could be a competing effect between the NO dissociation rate and the N_2 production rate. In fact, by varying the relationship between these two rates it was found that if the NO-dissociation rate value is smaller than or equal to the N_2 production one, sustained oscillations are obtained, in turn, if the NO dissociation rate is larger than the N_2 production rate, modulated oscillations are obtained.

It is important to mention that in all the previously analyzed situations the stoichiometry between CO_2 and N_2 is always maintained, as it is observed in Fig. 2(a).

The conditions described in the above situations are crucial for observing the existence or the inexistence of different oscillatory patterns. We now study how this oscillatory behavior can be affected by other variables. For instance, CO diffusion is a very important factor in our analysis. When we have included CO diffusion, clear oscillations are produced. If the CO diffusion rate constant increases, the amplitudes and periods of oscillations become longer, due to the fact that CO is being moved on the surface and that this diffusion is not hindered by phase boundaries. In consequence CO nuclei are formed slowly, and thereby the hex$\rightarrow1\times1$ transformation is slow too. This fact was also observed in simulations performed by Zhdanov for the NO reduction by CO (Ref. 10) as well as in the CO oxidation on a Pt(100) surface.[21] Figure 4 shows the oscillatory behavior for different rate constants of the CO diffusion process. On the other hand, if NO diffusion is neglected, this does not affect qualitatively the results, but if it is taken into account, then, when the rate of NO diffusion is equal to that of CO diffusion, oscillations amplitudes are the same and oscillations periods are shorter; how-

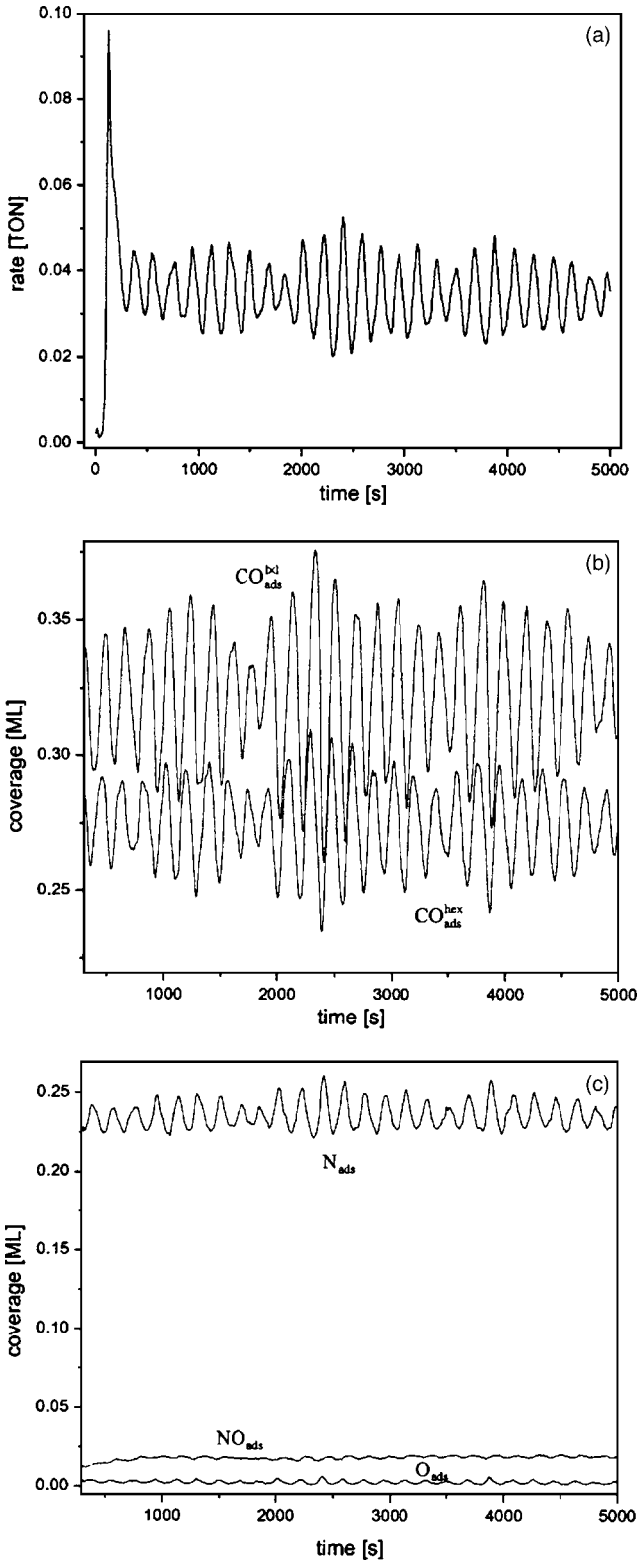

FIG. 3. Modulated oscillations: (a) CO_2 reaction rate for $W_{NOdis} \approx 50\ s^{-1}$; (b) CO coverage on square and hexagonal phases; (c) NO, N, and O coverages. Grid size: 256×256 unit cells.

ever, if the rate of NO diffusion is larger than that of CO diffusion, then oscillations amplitudes are smaller and the oscillations periods are shorter.

The appearance of the observed kinetic oscillations is possible due to the existence of a synchronized mechanism, which can be explained as follows. The simulation is started

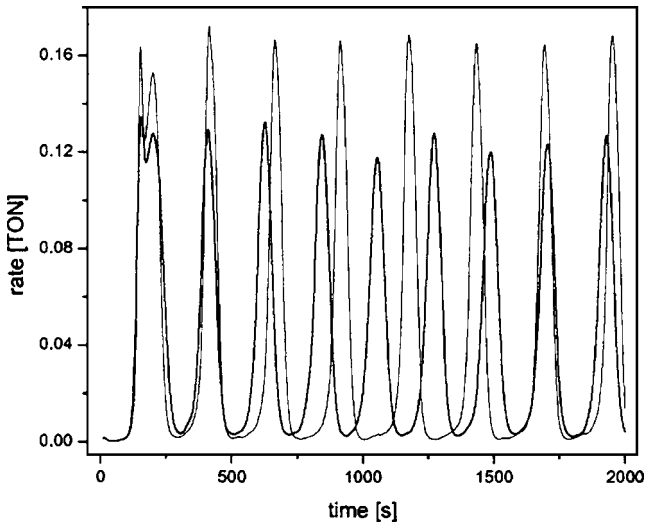

FIG. 4. Sustained oscillations. Thick lines correspond to $W_{COdif} = 10\ s^{-1}$ and thin lines to $W_{COdif} = 50\ s^{-1}$, respectively. Grid size: 256×256 unit cells.

with an empty grid of the hexagonal phase, on which only CO is adsorbed. As time passes small nuclei are formed and with a certain probability these will transform small portions of the surface into the square phase, next this phase grows by trapping reactions, such process is known as the *transformation stage*. When a CO molecule desorbs from the square phase surface, it leaves a vacant unit cell and then a NO molecule from the gas phase can be adsorbed hereon, since the NO adsorption rate is larger that the CO adsorption rate, then the unit cell will be preferentially occupied by NO. If another CO molecule desorbs from the same phase surface and if this vacant unit cell has a nn adsorbed NO, then this NO admolecule has the chance of dissociating. If this reaction is accomplished, then the adsorbed oxygen atoms can react with adsorbed CO while, in turn, adsorbed N atoms can react with adsorbed NO molecules thus forming the $(N–NO)^*$ intermediate. The formed species desorb in the form of molecular CO_2 and N_2 into the gas phase. Additionally, new empty unit cells are formed on the surface then allowing more NO molecules to adsorb; these molecules can later dissociate or react. Therefore, a *reactive stage* is created on the surface; experimentally this is known as "surface explosion"[3,5–7] and is only observed on the 1×1 phase. Also, the vacant unit cells existing on the square phase have a finite probability to undergo $1 \times 1 \rightarrow$ hex reconstruction, then small areas of the surface can go back slowly to the hexagonal configuration, this process is known as the *recovery stage*. Since NO cannot adsorb on the hexagonal phase, CO nuclei will be formed once more and the oscillation cycle will start again with the transformation stage. This synchronized mechanism is similar to that proposed by Gelten *et al.* for the CO oxidation.[22] Figure 5 shows snapshots of the surface evidencing the synchronized mechanism for a simulation grid that involves 1024×1024 unit cells. When the reaction stage is sufficiently advanced [Fig. 5(d)] a turbulence pattern is obtained for regions where O is reacting to form CO_2, immersed in disperse regions where N is reacting. This pattern type has been observed both experimentally and in other simulations.[2,10,22]

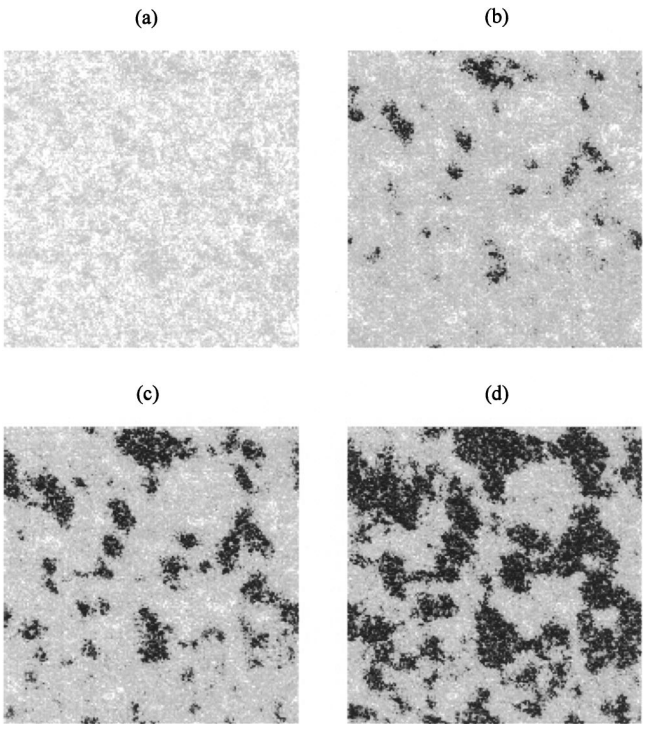

FIG. 5. Snapshots of the synchronized mechanism: (a) transformation stage at 90 s, (b) reactive stage at 115 s, (c) reactive stage at 120 s, and (d) reactive stage near the maximum, at 125 s. White sites stand for vacant H sites, CO adsorbed on H sites, vacant S sites, CO adsorbed on S sites, and NO adsorbed on S sites; gray sites stand for N adsorbed on S sites; black sites stand for O adsorbed on S sites.

We have also observed that when the $1\times1\rightarrow$hex transformation rate is increased or decreased by a factor of 4, the oscillations disappear. In fact, when the rate constant is increased, on the surface there exists too much of CO and too few of O species adsorbed, so the quantity of oxygen is not enough for the whole CO to be consumed. Now, if the rate constant is decreased, the converse case occurs, i.e., on the surface the adsorbed O atoms are in excess and there are few CO adsorbed, so that the square phase cannot go back to the hexagonal phase, thus terminating the synchronized mechanism.

Considering the same rate constants for the nucleation and trapping reactions and if these rates are increased by a factor of 6, then damped oscillations can be obtained. If these rates turn to be large enough, the oscillations can end since when the rate constants increase the hex$\rightarrow1\times1$ reconstruction becomes very fast and the recovery stage is not observed any more. On the other hand, if the rate constants are decreased by a factor of 3, the oscillations stop likewise since the hex$\rightarrow1\times1$ transformation is not completed; on the hexagonal phase there are small CO-islands blocking the recovery stage that started on the square phase, and this breaks down the synchronized mechanism.

Finally, we studied the effect of the grid size on the oscillation behavior as well as on the spatiotemporal patterns. When we have grids of 32×32 and 64×64 unit cells oscillations are not well defined, but with grids of 128×128 or more unit cells sharp oscillations are produced. The clearest spatiotemporal pattern formation is observed with large grids (1024×1024 unit cells or more).

IV. CONCLUSIONS

In this study an alternative reaction mechanism has been introduced in order to describe the catalytic conversion of NO+CO mixtures on the Pt(100) surface. This study takes into account the evidence gathered from recent experimental results of the same reaction performed on the Rh(111) surface. In this case, the nitrogen recombination step, that has been typically assumed to be responsible for the N_2 production, was replaced by a new mechanistic step that considers the formation of a $(N–NO)^*$ intermediary species. This activated complex decomposes eventually to $N_{2(gas)}$ and $O_{(ads)}$. In this way, by using a nonclassical mechanism, we have obtained different oscillatory patterns, namely, sustained, damped, modulated, and irregular, each one depending on the values of the different elementary step rates used to describe the kinetics of the system: mainly CO and NO adsorption-desorption, NO dissociation, and CO diffusion. The observed modulated oscillations represent a novel behavior in this reaction, which is not due to the introduction of an additional negative feedback loop but to the replacement of the classical N+N recombination step by the alternative $(N–NO)^*$ intermediary formation and decay step. A synchronization mechanism, as well as the formation of spatiotemporal patterns, arise when sustained oscillations occur.

ACKNOWLEDGMENTS

Financial support and scholarship to S.J.A. from the Consejo Nacional de Ciencia y Tecnología (CONACyT, México) is gratefully acknowledged. The authors would like to thank for the support of CONACyT-CONICET through the cooperation project "Catálisis, Fisicoquímica de Superficies e Interfases Gas-Sólido" between Mexico and Argentina.

[1] S. B. Schwartz and L. D. Schmidt, Surf. Sci. **206**, 169 (1988).
[2] G. Veser and R. Imbihl, J. Chem. Phys. **100**, 8483 (1994); **100**, 8492 (1994).
[3] Th. Fink, J.-P. Dath, R. Imbihl, and G. Ertl, J. Chem. Phys. **95**, 2109 (1991).
[4] R. Imbihl and G. Ertl, Chem. Rev. (Washington, D.C.) **95**, 697 (1995).
[5] Th. Fink, J.-P. Dath, M. R. Bassett, R. Imbihl, and G. Ertl, Vaccine **41**, 301 (1990).
[6] Th. Fink, J.-P. Dath, R. Imbihl, and G. Ertl, Surf. Sci. **251**, 985 (1991).
[7] Th. Fink, J.-P. Dath, M. R. Bassett, R. Imbihl, and G. Ertl, Surf. Sci. **245**, 96 (1991).
[8] G. Veser, F. Mertens, A. S. Mikhailov, and R. Imbihl, Phys. Rev. Lett. **71**, 935 (1993).
[9] N. Khrustova, G. Veser, A. Mikhailov, and R. Imbihl, Phys. Rev. Lett. **75**, 3564 (1995).
[10] V. P. Zhdanov, J. Chem. Phys. **110**, 8748 (1999).
[11] N. Hartmann, Y. Kevrekidis, and R. Imbihl, J. Chem. Phys. **112**, 6795 (2000).
[12] B. Meng, W. H. Weinberg, and J. W. Evans, J. Chem. Phys. **101**, 3234 (1994).
[13] M. Tammaro and J. W. Evans, J. Chem. Phys. **108**, 7795 (1998).
[14] O. Kortlüke, V. N. Kuzovkov, and W. von Niessen, Phys. Rev. Lett. **81**, 2164 (1998).
[15] K. Binder, *Monte Carlo Methods in Statistical Physics* (Springer, Berlin, 1986).
[16] F. Zaera and C. S. Gopinath, J. Chem. Phys. **111**, 8088 (1999).
[17] F. Zaera and C. S. Gopinath, Chem. Phys. Lett. **332**, 209 (2000).

[18]C. S. Gopinath and F. Zaera, J. Phys. Chem. B **104**, 3194 (2000).
[19]F. Zaera, S. Wehner, C. S. Gopinath, J. L. Sales, V. Gargiulo, and G. Zgrablich, J. Phys. Chem. B **105**, 7771 (2001).
[20]V. Bustos, C. S. Gopinath, R. Uñac, F. Zaera, and G. Zgrablich, J. Chem. Phys. **114**, 10927 (2001).
[21]F. Zaera and C. S. Gopinath, J. Chem. Phys. **116**, 1128 (2002).
[22]R. J. Gelten, A. P. J. Jansen, R. A. van Santen, J. J. Lukkien, J. P. L. Segers, and P. A. J. Hilbers, J. Chem. Phys. **108**, 5921 (1998).
[23]J. J. Lukkien, J. P. L. Segers, P. A. J. Hilbers, R. J. Gelten, and A. P. J. Jansen, Phys. Rev. E **58**, 2598 (1998).
[24]Y. Y. Yeo, L. Vattuone, and D. A. King, J. Chem. Phys. **104**, 3810 (1996).
[25]R. J. Behm, P. A. Thiel, P. R. Norton, and G. Ertl, J. Chem. Phys. **78**, 7437 (1983); **78**, 7448 (1983).
[26]T. E. Jackman, K. Griffiths, J. A. Davies, and P. R. Norton, J. Chem. Phys. **79**, 3529 (1983).
[27]P. A. Thiel, R. J. Behm, P. R. Norton, and G. Ertl, Surf. Sci. **121**, L553 (1982).
[28]Y. Y. Yeo, C. E. Wartnaby, and D. A. King, Science **268**, 1731 (1995).
[29]A. Hopkinson, J. M. Bradley, X. C. Guo, and D. A. King, Phys. Rev. Lett. **71**, 1597 (1993).
[30]M. A. Barteau, E. I. Ko, and R. J. Madix, Surf. Sci. **102**, 99 (1981).
[31]J. Ross and M. O. Vlad, Annu. Rev. Phys. Chem. **50**, 51 (1999).